Intelligent Automation & Soft Computing

ISSN: 1079-8587 (Print) 2326-005X (Online) Journal homepage: http://www.tandfonline.com/loi/tasj20

An enhanced representation of thermal faces for improving local appearance-based face recognition

Gabriel Hermosilla, Javier Ruiz-del-Solar & Rodrigo Verschae

To cite this article: Gabriel Hermosilla, Javier Ruiz-del-Solar & Rodrigo Verschae (2015): An enhanced representation of thermal faces for improving local appearance-based face recognition, Intelligent Automation & Soft Computing, DOI: 10.1080/10798587.2015.1110288

To link to this article: http://dx.doi.org/10.1080/10798587.2015.1110288

Published online: 14 Dec 2015.

INTELLIGENT AUTOMATION AND SOFT COMPUTING, 2015
http://dx.doi.org/10.1080/10798587.2015.1110288

An enhanced representation of thermal faces for improving local appearance-based face recognition

Gabriel Hermosilla[a], Javier Ruiz-del-Solar[b,c] and Rodrigo Verschae[c]

[a]Pontificia Universidad Católica de Valparaíso, Valparaíso, Chile; [b]Department of Electrical Engineering, Universidad de Chile; [c]Advanced Mining Technology Center, Universidad de Chile

ABSTRACT

This paper proposes a new methodology to improve appearance-based thermal face recognition methods by using an enhanced representation of the thermal face information. This new representation is obtained by combining the pixels of the thermal face image and the vascular network information that is extracted from the same thermal face image. The effect of using the enhanced representation is evaluated for 5 different face recognition methods (LBP, WLD, GABOR, SIFT, SURF) in two public thermal face databases (Equinox and UCHThermalFace). The experimental results show that the proposed enhanced representation improves the performance of most of the analyzed appearance-based methods. The largest improvements are obtained when this representation is used together with methods based on the Gabor Jet Descriptor (GJD), the Weber Linear Discriminant (WLD) and Speeded Up Robust Features (SURF). In general terms the improvement is larger in indoor setups than in outdoors.

KEYWORDS

Face recognition; thermal face recognition; unconstrained environments; vascular network

1. Introduction

The recent progress in infrared technology allows its use in several applications in a much simpler and efficient way than before. The technology has attracted the attention of researchers due to improvements in the acquisition technology and a significant decrease in costs. This field has seen steady growth due to its several applications (Gade & Moeslund, 2014), including security (e.g. access and identity control (Wong, Tan, Loo, & Lim, 2009), energy efficiency (e.g. detection of defective thermal insulation (Vidas, Moghadam, & Bosse, 2013)), and health care (e.g. breast cancer detection (Qi & Diakides, 2009)). In the particular case of face recognition applications, its use allows to address limitations of visual cameras associated to variable illumination conditions and changes in the head pose (Socolinsky & Selinger, 2002).

Existing thermal face recognition methods can be roughly grouped into three main categories:

(i) *Appearance based* methods that analyze the image pixels using methodologies that are similar to the ones used in standard—visible-spectrum—face recognition (appearance based, local matching, global matching, etc.; see for example (Chen, Flynn, & Bowyer, 2003; Hermosilla, Ruiz-del-Solar, Verschae, & Correa, 2012; Méndez, San Martín, Kittler, Plasencia, & García-Reyes, 2009; Socolinsky & Selinger, 2002; Socolinsky & Selinger, 2004; Socolinsky, Wolff, Neuheisel, & Eveland, 2001).

(ii) *Vascular information-based* methods that use vascular information, obtained by detecting thermal gradients, for characterizing and analyzing the face data (Buddharaju & Pavlidis, 2007; Buddharaju, Pavlidis, & Manohar, 2008; Buddharaju, Pavlidis, & Tsiamyrtzis, 2005; Buddharaju, Pavlidis, & Tsiamyrtzis, 2006; Cho, Wang, & Ong, 2009).

(iii) *Combined visible and thermal* methods that combine the analysis of visible and thermal images in order to carry out the recognition (Bebis, Gyaourova, Singh, & Pavlidis, 2006; Desa & Hati, 2008; Pop, Gordan, Florea, & Vlaicu, 2010).

One of the most comprehensive comparative studies of thermal face recognition methods was recently presented in (Hermosilla et al., 2012). The methods in that study were selected considering that they fulfill the following requirements: (a) No offline enrollment / modeling stages, (b) real-time processing, (c) single sample per person (one thermal face image per subject in the gallery), and (d) no restrictions on the environmental data acquisition conditions. The study analyzed in particular the effect of face alignment, occlusions, face size, face expressions, and indoor/outdoor illumination in the recognition process. The analyzed methods were histograms of Local Binary Pattern (LBP) features (Ahonen, Hadid, & Pietikainen, 2006), Gabor Jet Descriptors (GJD) with Borda count classifiers (Zou, Ji, & Nagy, 2007), histograms of Weber Linear Descriptor (WLD) features (Chen et al., 2010), Scale-Invariant Feature Transform (SIFT) image-matching (Lowe, 2004), and Speeded Up Robust Features (SURF) image-matching (Bay, Ess, Tuytelaars, & Van Gool, 2008). In general terms, all compared methods obtained a good performance under those unconstrained conditions, and no method was consistently better that the others when considering recognition performance and processing speed at the same time.

The main goal of this paper is to present a new methodology that allows improving thermal face recognition methods by using an enhanced thermal representation of the

CONTACT Gabriel Hermosilla gabriel.hermosilla@pucv.cl

faces, representation that can be used with any standard face recognition method. This new representation is obtained by combining the pixels of the thermal face image with vascular network information that is extracted from the same thermal face image (see an example of this enhanced representation in Figure 2 (e)). By enhancing the way in which the thermal face information is represented, the recognition performance of thermal face recognition methods, such as the ones analyzed in (Hermosilla et al., 2012), can be improved. Hence, a new family of thermal face recognition methods that uses this enhanced representation is obtained: e-LBP, e-GJD, e-WLD, e-SIFT and e-SURF (*e* stands for enhanced). We focus on analyzing improvements produced by the use of this representation on local appearance methods that use only thermal images.

Fusing or combining information can be done at different levels (see e.g. (James & Dasarathy, 2014; Mangai, Samanta, Das, & Chowdhury, 2010; Nigam, Vatsa, & Singh, 2015)): Pixel, feature, and decision level. The pixel level fusion combines two images from different sources or sensors into a single resulting image, and this is done independently of the recognition method. The feature (or image descriptor) level fusion combines the descriptors, and thus it can only be applied together with methods that assume a higher-level representation (e.g. feature vector), and that do not work directly with images. The decision level fusion combines the output of dissimilarity measures (or different recognition methods), and therefore can be applied to combine existing recognition methods. In this paper we propose an enhanced image representation obtained by fusing information at the pixel levels, and therefore can be operate with any standard face recognition method.

In order to generate recognition results that are fully comparable with previous works, the proposed methodology is analyzed and validated using the Equinox (Equinox, 2012) and UCHThermalFace (UCHThermalFace, 2014) databases. These databases are public and have been used in the past (see for example the comparative studies presented in (Hermosilla et al., 2012; Socolinsky & Selinger, 2002). All methods analyzed in (Hermosilla et al., 2012) are compared here to their *e*-variants, i.e. to the here proposed methodology.

The paper is structured as follows: The related work is presented in Section 2. In Section 3 the proposed methodology is described. In Section 4 this methodology is analyzed (standard methods are compared to their corresponding *e*-variants) in the Equinox and UCHThermalFace databases. Finally, conclusions of this work are presented in Section 5.

2. Related work

Thermal face recognition has attracted increasing interest in the research community (see (Shoja Ghiass, Arandjelović, Bendada, & Maldague, 2014) for a recent review), and several comparative studies of thermal face recognition methods have been developed in recent years (Hermosilla et al., 2012; Socolinsky & Selinger, 2002; Socolinsky et al., 2001). Existing thermal face recognition methods can be roughly classified into three main categories: *Appearance based* methods (Hermosilla et al., 2012; Méndez et al., 2009; Socolinsky & Selinger, 2002; Socolinsky et al., 2001), *vascular information based* methods (Buddharaju & Pavlidis, 2007; Buddharaju et al., 2006; Cho et al., 2009), and *combined visible and thermal* methods (Bebis et al., 2006; Desa & Hati, 2008; Pop et al., 2010).

The methods in the last category are used mainly to overcome some of the drawbacks of using thermal images, mainly the opaqueness of eyeglasses in the thermal spectrum and the dependence of thermal images to the environmental temperature and the internal state of the subjects (emotional, health and physical conditions) (Shoja Ghiass et al., 2014). However, the obvious limitation of this approach is the need of having thermal and visible spectrum face images at the same time. Any thermal face recognition method can be complemented with face recognition methods working in the visible spectrum; therefore, we will concentrate in thermal face recognition in this analysis.

The performance of any face recognition method depends on the particular conditions under which the images are captured, and thus different databases can be used to measure different issues. The most popular database for thermal face recognition studies is Equinox (Equinox, 2012), even though it considers limited environmental conditions (variations in illumination and facial expressions). Using Equinox, the best reported performance are obtained by the WLD and LBP standard face recognition approaches, achieving a ~99% recognition rate (Hermosilla et al., 2012). When a database that considers more realistic environmental conditions, such as the UCHThermalFace (UCHThermalFace, 2014) database is used, the best performing methods are the ones based on SIFT and WLD. SIFT achieves the highest recognition rate, while WLD gets the best tradeoff between recognition rate and processing speed.

Most of the works that use the vascular information for thermal face recognition are based on the works of Buddharaju *et al.*, where the vascular representation is calculated by detecting thermal minutia points, and then matching them using an approach similar to the ones used for fingerprint identity verification (Buddharaju & Pavlidis, 2007; Buddharaju et al., 2005; Buddharaju et al., 2006; Buddharaju et al., 2008). This methodology achieves a ~80% recognition rate in the University of Notre Dame database. In (Cho et al., 2009) a similar approach based on thermal *faceprints* is proposed. This approach uses a new feature for representing the thermal face image: The bifurcation points of the thermal pattern and the center of gravity of the thermal face region. In (Ghiass, Arandjelovic, Bendada, & Maldague, 2013a; Ghiass, Arandjelovic, Bendada, & Maldague, 2013b) the use of Active Appearance Model (AAM) is introduced for improving the vascular matching, in addition to use a non-binary representation of the vascular information, achieving a 100% recognition rate in the University of Houston database. In (Mostafa, Hammoud, Ali, & Farag, 2013) a face recognition method for low-resolution thermal images is presented. The method uses a texture detector based on Haar features and Adaboost for the automatic alignment of images, and LBP, SIFT and BRIEF as facial signatures, and it was evaluated in the University of Notre Dame database. In (Zheng, 2010; Zheng & Elmaghraby, 2011) the recognition of thermal faces using Gabor wavelets, as the base of the Face Pattern Byte (FPB) method, is addressed. FPB is compared with PCA, LDA and EBGM-based systems using the ASUMS face database. In (Hanmandlu, 2014) a thermal face authentication system that uses information set based features and statistical classifiers is proposed.

To the best of our knowledge, there is no previous works reporting the combined use of appearance *based* and *vascular information based* approaches.

3. Enhanced thermal face representation

As mentioned, our main contribution is an enhanced representation of the thermal information, representation that

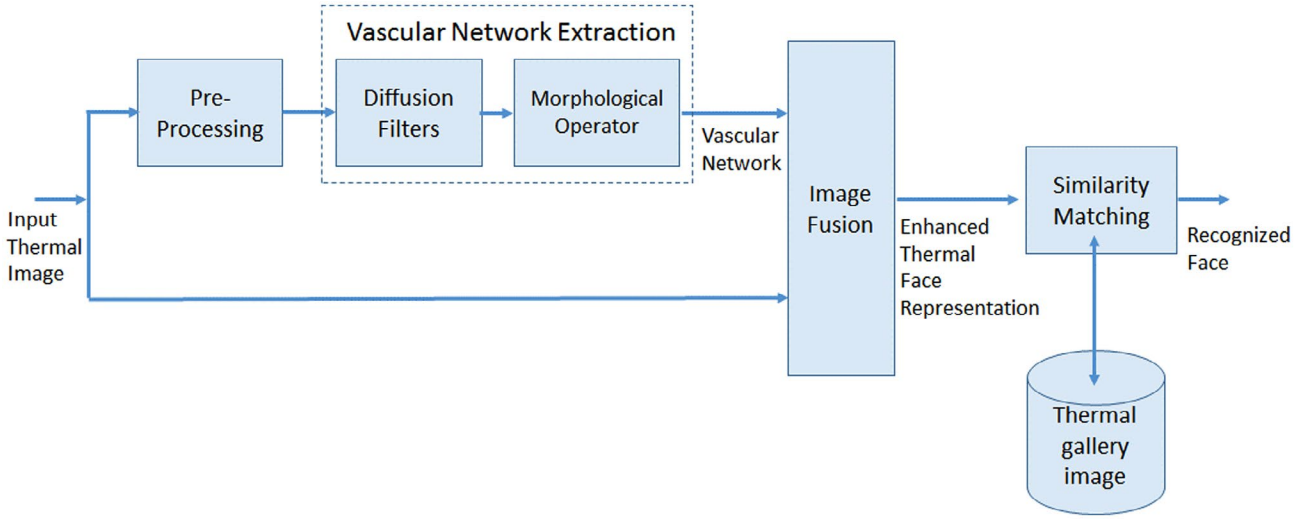

Figure 1. Block Diagram of the Proposed Methodology.

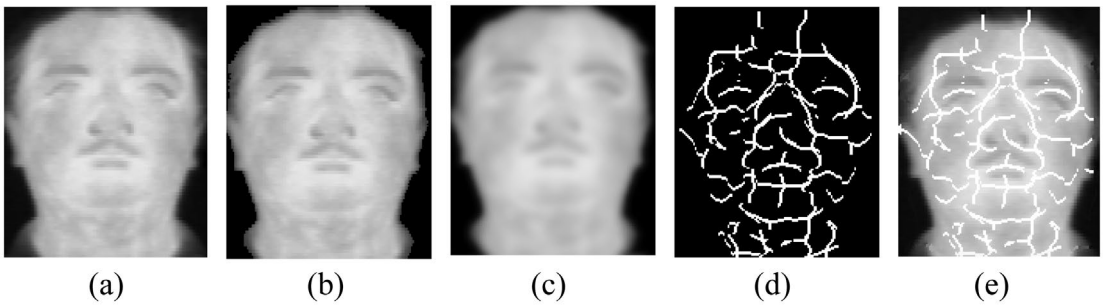

Figure 2. Example Results of the Steps for Extracting the Enhanced Thermal Face Representation.
(a) Input Thermal Image, (b) Segmented Face, (c) Filtered Face Using Anisotropic Diffusion, (d) Vascular Network, (e) Enhanced Thermal Face Representation.

can be used with any standard face recognition method. By extracting information of the face's vascular network from the thermal face image[1], and by combining that information with the thermal face image for its use in the recognition of the faces, the enhanced representation is obtained. The proposed method consists of three main stages:

- Thermal face preprocessing (e.g. segmentation),
- Vascular network information extraction, and
- Fusion of the vascular network and the thermal face image.

A simplified diagram of the process is presented in Figure 1, and an example result of the intermediate steps is presented in Figure 2. After the enhanced thermal face image is obtained, any appearance-based face recognition method can be applied. Thus, the thermal image enhancement can be thought of as a pre-processing step to be applied prior to the recognition of the faces. The enhanced representation, though very simple, is effective for improving the performance of some face recognition methods, as will be shown in Section 4. In addition, it has a low processing overhead. In the following we describe the process to obtain the *enhanced thermal face representation*.

3.1. Thermal face preprocessing

The thermal image of a face (see Figure 2(a) for an example) is segmented from the background by means of probability models of the grayscale distribution of the face and non-face pixels. The probability of a pixel x of being part of a face, and the probability of it being a non-face pixel are modeled using Gaussian distributions, as follows:

$$p(x|c) = \frac{1}{\sqrt{2\pi}\sigma_c} \exp\left(-\frac{1}{2}\frac{(x-\mu_c)^2}{\sigma_c^2}\right), \qquad (1)$$

where x represents the grey-scale intensity of a pixel, and $c \in \{\text{face, non - face}\}$ the class of the pixel. These probability distributions are estimated using an approach similar to the one introduced in (Jones & Rehg, 2002) for the segmentation of skin in the visible spectrum.

Let us call $I_{thermal}$ the input thermal image of size *WxH pixels* and let us call $\Omega = \{(i,j)|1 \le i \le W, 1 \le j \le H\}$ the support of the image. We use the just described probability model to determine if pixel *(i,j)* of $I_{thermal}$ corresponds to the background or to the face:

$$I_{mask}(i,j) = \begin{cases} 1 & if \ \frac{p(I_{thermal}(i,j)|\text{c=face})}{p(I_{thermal}(i,j)|\text{c=nonFace})} < th_{mask} \\ 0 & otherwise \end{cases} \qquad (2)$$

With th_{mask} the decision threshold. In other words, the ratio of the probabilities are compared against a given threshold, obtaining a binary mask I_{mask} indicating which pixels belong to the thermal face image.

Using the obtained binary mask, the segmented image, I_{seg}, is obtained by point-wise multiplying the thermal image and the mask image (see Figure 2 (b) for an example):

$$I_{seg}(i,j) = I_{thermal}(i,j) \cdot I_{mask}(i,j) \qquad \forall (i,j) \in \Omega \qquad (3)$$

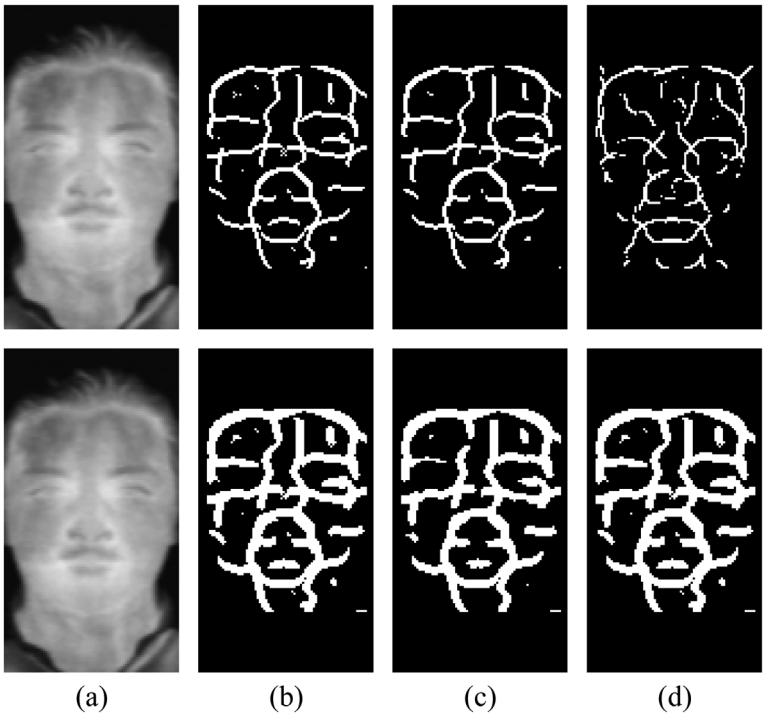

Figure 3. Example Results of Vascular Network Obtained Using Different Structural Elements.
First/Second Row: Structural Element of $3\times3/5\times5$ Pixels. (a) Original Image, (b) Square-shape Structural Element, (c) X-shape Structural Element, and (d) Disk-shape Structural Element.

3.2. Vascular network information extraction

In order to extract information of the vascular network diffusion filters and, morphological operators are used. First, an anisotropic diffusion filtering is used to enhance the areas where a large amount of heat is detected by means of an iterative process applied over the segmented image. Following the procedure proposed in (Buddharaju et al., 2008), where, at iteration $t = 1, ..., T$, a filtered (smoothed) image is calculated as:

$$I_{sm,t+1}(i,j) = I_{sm,t}(i,j) + \frac{1}{4}\sum\nolimits_{d\in\Delta} c_{d,t}(i,j)\nabla I_{d,t}(i,j) \quad (4)$$

with $I_{sm,0}(i,j) = I_{seg}(i,j)$, and $\Delta = \{N, E, S, W\}$ the direction of the filters (north, south, west and east; respectively), and $\nabla I_{d,t}(i,j)$ the gradient at (i,j) for direction $d \in \Delta$. The gradients are estimated using differences between neighbor pixels:

$$\begin{aligned}
\nabla I_{N,t}(i,j) &= I_{\mathrm{sm},t}(i,j+1) - I_{\mathrm{sm},t}(i,j)\\
\nabla I_{S,t}(i,j) &= I_{\mathrm{sm},t}(i,j) - I_{\mathrm{sm},t}(i,j-1)\\
\nabla I_{E,t}(i,j) &= I_{\mathrm{sm},t}(i+1,j) - I_{\mathrm{sm},t}(i,j)\\
\nabla I_{W,t}(i,j) &= I_{\mathrm{sm},t}(i,j) - I_{\mathrm{sm},t}(i-1,j)
\end{aligned} \quad (5)$$

The four diffusion coefficients in Eq. (4), corresponding to the north, south, west, and east directions, depend on the squared gradients and are computed as:

$$c_{d,t}(\mathrm{i},\mathrm{j}) = \exp\left(-\frac{\nabla I^2_{d,t}(i,j)}{k^2}\right) \quad (6)$$

With k a constant empirically set to 100. Note that Eqs. (4)-(6) cannot be used on pixels in the borders of the image; in those cases the gradients are set to zero when computing the filtered image.

After T iterations the filtered (smoothed) image is obtained: $I_{\mathrm{filtered}}(i,j) = I_{sm,T}(i,j)$ (see Figure 2 (c) for an example). The number of iterations of the diffusion filter was set empirically to $T = 10$.

Once the filtered image has been obtained, a "Top Hat" segmentation (Buddharaju et al., 2008) is applied. This procedure consists of applying an erosion operator followed by a dilation operator:

$$I_{open} = (I_{filtered} \odot S) \oplus S \quad (7)$$

with S a structural element, $\odot$ the erosion and $\oplus$ the dilation morphological operators, respectively. Finally, the image containing information of the vascular network, $I_{vascular}$, is obtained by subtracting the filtered image and the image obtained from the Top-Hat-Segmentation:

$$I_{vascular} = I_{filtered} - I_{open} \quad (8)$$

After obtaining the vascular image $I_{vascular}$ and binary image containing the vascular network is obtained by applying a threshold, $th_{vascular}$ to the vascular $I_{vascular}$. We call this image I_{vn}. See Figure 2 (d) for an example of an extracted vascular network obtained using a threshold value equals to $th_{vascular} = 0$.

3.2.1. Selection of the Structural Element

Three different structural elements for the erosion and dilation morphological operations, during top hat segmentation, were analyzed: Square-shape, x-shape, and disk-shape. In each case, two sizes were considered for the support region: 3×3 and 5×5. Equation (9) shows the 3 structural elements for the 3×3 case (the 5×5 elements are similar, but have larger support).

$$S_{square} = \begin{pmatrix} 1 & 1 & 1\\ 1 & 1 & 1\\ 1 & 1 & 1 \end{pmatrix} S_x = \begin{pmatrix} 1 & 0 & 1\\ 0 & 1 & 0\\ 1 & 0 & 1 \end{pmatrix} S_{disk} = \begin{pmatrix} 0 & 1 & 0\\ 1 & 1 & 1\\ 0 & 1 & 0 \end{pmatrix}. \quad (9)$$

Several face images were processed using the different structural elements, and the obtained results were carefully analyzed (see some examples in Figure 3). It was observed that the 5×5 sized elements do not seem to add much information compared to the 3×3 ones, other than connecting/disconnecting some part of the vascular network (see for example the forehead in Figure 3). When comparing the results for different shapes, we could observe that the square-shape and the x-shape give very similar results, but the x-shaped element produces less noise. It is also interesting to observe that the x-shape and the square-shape gave similar results in terms of their topology, but in the case of the disk-shape the topology is rather different, with the 3×3 disk-shape extracting mainly diagonal structures. Given that (i) the x-shape gives less noise, (ii) the topology of the network it generates is more stable (thus it is less independent of the size of structural element), and (iii) the analyzed face recognition methods are not based on the connectivity of the network, nor on fiducial points, we decided to use the x-shaped element with a 3×3 support region in the reported experiments.

3.2.2. Thermal Face Image normalization

After processing several thermal images from different sources, it was observed that some images have low contrast, and they need to be pre-processed before applying the anisotropic diffusion. This happens for instance in the case of the Equinox database images. In those cases, an additional step is required before performing the vascular network extraction, which consist on normalizing by applying a linear mapping of the pixels intensity values to the range $[N_{min}, N_{max}]$:

$$I_{norm}(i,j) = \frac{I(i,j) - I_{\min}}{I_{\max} - I_{\min}}\left(N_{max} - N_{min}\right) + N_{min} \qquad \forall (i,j) \in \Omega, \tag{10}$$

with I_{min} and I_{max} the minimum and maximum values in the image: $I_{min} = min_{(i,j\in\Omega}I_{(i,j)}$ and $I_{max} = \max_{(i,i)\in\Omega} I(i,j)$. In the experiments the values $N_{min} = 0$ and $N_{max} = 255$ were used. In the case of the UCHThermalFace normalizing the histogram was not necessary because the images already have a histogram that almost covers the whole range [0,255]. On the contrary, the images in the Equinox database come in a 12-bit format, with most image with values in the range [1,500-2,500], thus the normalization step was needed.

3.3. Fusion of the vascular network and the thermal face image

For combining the thermal image and the vascular network image a simple, yet general framework, is proposed. The basic idea is to combine the images in a way that the vascular information is emphasized in the original thermal image, without losing the appearance information of the thermal face image. For this, the enhanced image is obtained by taking the thermal image and the vascular and combining them using a fusion operator:

$$I_e = op(I_1, I_2), \tag{11}$$

that in this case takes two input images ($I_1 = I_{thermal}$ and $I_2 = I_{vn}$) of the same size, and combines them applying pixel-wise operations. Several such operators exists, and we consider the Ordered Weighted Averaging (OWA) operator (Yager, 1988), which takes a sequence of values, sorts them, and calculates the ordered weighted values. If there are n values, $p_1, p_2, \ldots p_n$, the OWA operator combines them as $p = \Sigma_k w_k p_{(k)}$, with $p_{(k)}$ the k-th smallest value in $p_1, p_2, \ldots p_n$. In our case, the OWA operator works only on two values (two pixels, one from each image). However, the proposed method could also be used together with other sources of information, such as depth images, other infrared bands, and/or visual images. Let us call $p_1(i,j) = \min\left(I_1(i,j), I_2(i,j)\right)$, and $p_2(i,j) = \max\left(I_1(i,j), I_2(i,j)\right)$, then:

$$I_e(i,j) = w_1 p_1(i,j) + w_2 p_2(i,j), \tag{12}$$

with $\sum_{k=1}^{K} w_k = 1$. Using different values of w_k we can define different operations, for example when $w_k = \frac{1}{K}$ we have the average, while in the case $w_1 = 1$ we have the minimum, and in the case $w_K = 1$ the maximum among the K values. In our case $K=2$, thus we can easily define the maximum, minimum or any weighted sum between the two values. Examples of this fusion operator applied to images of the Equinox and UCHThermalFace database are shown in Figure 4. In the following section we will analyze the selection of such parameters, as well as the robustness of the proposed representation.

4. Evaluation

The proposed methodology is evaluated using the same methodology and data as in the comparative study done in (Hermosilla et al., 2012), study that uses the Equinox database (Equinox, 2012) and the UCHThermalFace database (UCHThermalFace, 2014). We consider the same methods and implementation used in (Hermosilla et al., 2012). We provide a very brief description of the used methods, and direct the reader to (Hermosilla et al., 2012) and the original papers for more details:

- **LBP Histograms**. In (Ahonen et al., 2006), histograms of LBP features for face recognition are used considering three different levels of locality: Pixel, regional, and holistic level. The input face image is partitioned into 10 (2×5), 40 (4×10), or 80 (4×20) regions (the size of each region depends on the size of the image), and from each region a histogram of LBP features is obtained and then the histograms are concatenated (for more details see (Ahonen et al., 2006; Ruiz-del-Solar, Verschae, & Correa, 2009). For recognition, a nearest neighbor classifier is used with three similarity measures: histogram intersection, log-likelihood statistic, or Chi-square.
- **Gabor Jet Descriptors**. Uniformly distributed Gabor Jet Descriptors, one wave-length apart, are used as local features in a multiscale fashion. The distance between Gabor jets from two images is calculated using a normalized inner products and the Borda-Count voting method is used to obtain the recognized face.
- **WLD Histograms.** The WLD descriptor (Chen et al., 2010) is inspired by Weber's Law, and consist of a two dimensional histogram of local excitation and orientation. A nearest neighbor classifier is used for classification using the following similarity measures: Histogram intersection, Euclidean distance, and Chi-square. As in LBP, images are divided in 10, 40 or 80 regions, and the obtained histograms are concatenated to build the feature vector (for more details on how the portioning is done see (Ahonen et al., 2006; Ruiz-del-Solar et al., 2009).

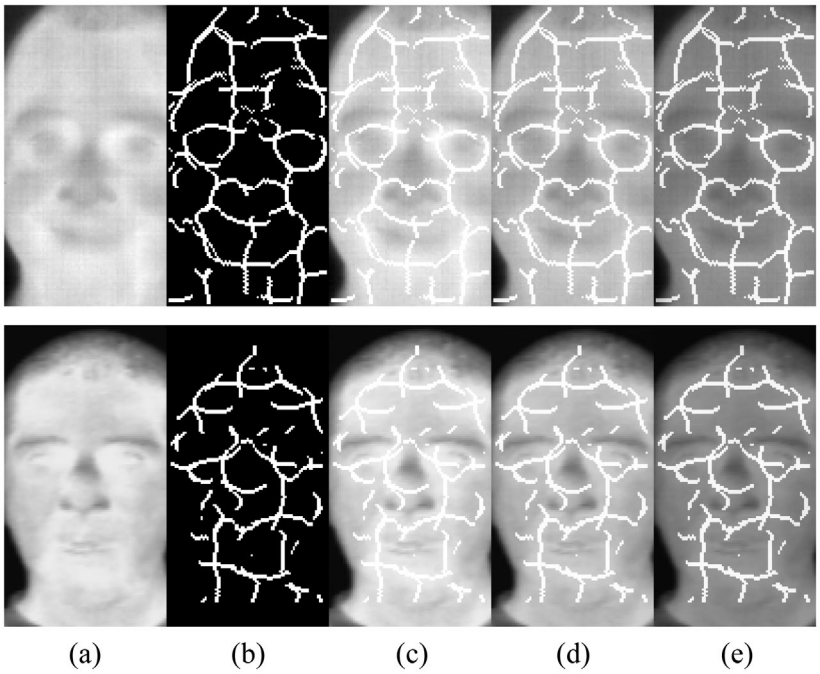

Figure 4. Example Results of the Fusion Operator Using Different wi Parameters.
Top: Image from the Equinox Database. Bottom: Image from the UCHThermalFace Database. From Left to Right: (a) Thermal Image, (b) Vascular Network Image, (c) Fusion Operator $(w_1 = 0, w_2 = 0.7)$, (d) Fusion Operator $(w_1 = 0.1, w_2 = 0.9)$, and (e) Fusion Operator $(w_1 = 0.3, w_2 = 0.7)$.

- **SIFT Descriptors**. Two variants of the SIFT wide-baseline matching approach are considered: The original Lowe's system (Lowe, 2004) for basic matching, and the L&R system (Ruiz-del-Solar, Loncomilla, & Devia, 2007) that adds hypothesis rejection. In both SIFT cases the numbers of matched key points are used to measure the similarity between two images (in the following we will refer to it as *matches*).
- **SURF Descriptors**. The SURF method (Bay et al., 2008) proposes to compute local interest points and descriptors at a higher speed than the SIFT approach by using a Fast-Hessian detector that approximates Gaussians filters and convolutions using box-filters and the integral image. The SURF descriptors consist of Haar-wavelets responses at the interest-point neighborhood. As in the SIFT-Lowe case, the number of matched descriptors is used as similarity measure (*matches*). The OpenSURF implementation provided by (Evans, 2009) is used.

We use the same notation as (Hermosilla et al., 2012) to refer to the methods and their variations: *XX-YY-ZZ*. (i) *XX* describes the name of the face-recognition algorithm: LBP, WLD, GJD, SIFT-Lowe (Lowe's system with SIFT descriptors), SIFT-L&R (L&R system with SIFT descriptors), and SURF; (ii) *YY* denotes the similarity measure or classification approach: HI (Histogram Intersection), XS (Chi square), EU (Euclidian Distance), BC (Borda Count), with exception of SIFT and SURF methods that do not use any explicit distance measure; (iii) *ZZ* describes additional parameters: Number of partitions in the case of the LBP-based and WLD-based methods, and matching method in the case of SIFT and SURF methods (M: number of matches; S: simple).

In the present work, for each method we consider the variant in (Hermosilla et al., 2012) with best performance: LBP-HI-80, GJD-BC, WLD-EU-80, WLD-HI-80, SIFT-L&R-M, SIFT-Lowe-M, and SURF-M. We use the following notation for indicating the case when these methods use the enhanced representation: e-LBP-HI-80, e-GJD-BC, e-WLD-EU-80, e-WLD-HI-80, e-SIFT-L&R-M, e-SIFT-Lowe-M, and e-SURF-M.

When using the Equinox database, the recognition experiments in (Hermosilla et al., 2012) and in the present work follow the same methodology as in (Socolinsky & Selinger, 2002; Socolinsky et al., 2001), where for each of the 54 gallery-test set experiments, the top-1 recognition rate is computed, and then the average performance over all the gallery-test set experiments is computed. Similarly, for the UCHThermalFace database, the same recognition experiments, and implementation of the recognition methods employed in (Hermosilla et al., 2012) are used. We now give a brief description of the experimental setups and direct the reader to (Hermosilla et al., 2012) for further reference:

- **The Equinox database** consists of 18,629 visible and thermal images (8–12 um) of 240 × 320 of resolution. The images correspond to 91 individuals consider different illumination conditions and expressions. Experiments were run considering different combinations of gallery-test sets, and for each experiment, the methods are evaluated by considering 1 image per individual in the gallery and thermal face images of size 81 × 150 pixels.
- **The UCHThermalFace** database (UCHThermalFace, 2014) consists of three sets: *Rotation, Speech* and *Expressions (53, 53 and 102 subjects respectively)*. The thermal images were acquired using a FLIR 320 TAU Thermal Camera, which has a sensitivity in the range 7.5 -13.5 μm, and a resolution of 324 × 256 pixels. We follow the procedure introduced in (Ruiz-del-Solar et al., 2009) and used (Hermosilla et al., 2012), which consist in evaluating the robustness of the methods to different difficulties appearing in face recognition problems, and we use the same windows sizes as in (Hermosilla et al., 2012) (the used window size is different for each method). The performed experiments are [2]
  - *Baseline case*: No variations applied to the images.
  - *Partial Face Occlusions* applied to the faces.

Table 1. Average top-1 Face Recognition Rate (%) for the Equinox Database when Different Representations are used.

Method	Standard Thermal Representation	Vascular Representation	Enhanced Face Representation(e-variants) $w_1=0$ $w_2=1$	Enhanced Face Representation(e-variants) $w_1=0$ $w_2=0$	Enhanced Face Representation(e-variants) $w_1=0.3$ $w_2=0.7$	Performance Improvement of obtained by the Enhanced Face Representation (e-variants) $w_1=0$ $w_2=1$	Performance Improvement of obtained by the Enhanced Face Representation (e-variants) $w_1=0.1$ $w_2=0.9$	Performance Improvement of obtained by the Enhanced Face Representation (e-variants) $w_1=0.3$ $w_2=0.7$
LBP-HI-80	92.68	86.20	**93.01**	92.43	91.68	**0.36**	−0.27	−1.08
GJD-BC	70.07	88.10	86.94	87.99	**88.22**	24.08	25.57	**25.90**
WLD-EU-80	84.17	80.49	**85.62**	85.57	85.25	**1.72**	1.66	1.28
WLD-HI-80	84.88	84.71	85.03	87.34	**87.64**	0.18	2.90	**3.25**
SIFT-L&R-M	70.25	57.95	79.32	**82.79**	77.38	12.91	**17.85**	10.15
SIFT-Lowe-M	76.97	70.62	84.37	**87.38**	85.35	9.61	**13.52**	10.89
SURF-M	52.14	79.30	71.90	77.48	**81.29**	37.90	48.60	**55.91**

The enhanced representation is obtained using different combinations of the w_i parameters, when applying the fusion operator. Best results for each method are shown in bold letters. The performance improvement represents the relative improvement achieved by the enhanced representation, calculated as $100(EFR - STR)/STR$, with SRT the face recognition rate of the standard thermal representation and efr the face recognition rate of the enhanced face representation.

Table 2. Average Top-1 Face Recognition rate (%) for the UCHThermalFace Database (Baseline Case) when Different Representations are used.

Method	Standard Thermal representation	Vascular representation	Enhanced Face Representation(e-variants) $w_1=0$ $w_2=1$	Enhanced Face Representation(e-variants) $w_1=0.1$ $w_2=0.9$	Enhanced Face Representation(e-variants) $w_1=0.3$ $w_2=0.7$	Performance Improvement of obtained by the Enhanced Face Representation(e-variants) $w_1=0$ $w_2=1$	Performance Improvement of obtained by the Enhanced Face Representation(e-variants) $w_1=0.1$ $w_2=0.9$	Performance Improvement of obtained by the Enhanced Face Representation(e-variants) $w_1=0.3$ $w_2=0.7$
LBP-HI-80	88.51	88.48	**89.11**	**89.11**	88.45	**0.68**	**0.68**	−0.07
GJD-BC	91.37	45.94	95.65	**95.91**	95.82	4.68	**4.97**	4.87
WLD-EU-80	**91.80**	82.73	91.80	91.80	69.07	0.00	0.00	−24.76
WLD-HI-80	91.54	86.96	**96.48**	**96.48**	96.28	**5.40**	**5.40**	5.18
SIFT-L&R-M	**95.11**	69.75	94.88	94.94	94.33	−0.24	−0.18	−0.82
SIFT-Lowe-M	**97.60**	74.73	96.31	95.79	94.94	−1.32	−1.85	−2.73
SURF-M	94.94	87.19	**96.66**	96.44	95.96	**1.81**	1.58	1.07

The enhanced representation is obtained using different combinations of the w_i parameters, when applying the fusion operator. Best results for each method are shown in bold letters. The performance improvement represents the relative improvement produced by the enhanced representation achieved by the enhanced representation, calculated as $100(EFR - STR)/STR$, with SRT the face recognition rate of the standard thermal representation and efr the face recognition rate of the enhanced face representation.

  - *Eye Detection Accuracy*: White noise is added to the position of the annotated eyes in the test images. The noise can be up to 2.5, 5, or 10% of the distance between the eyes
- *Indoor* versus *Outdoor Galleries*[3]
- *Facial Expressions.*

Using both databases, the performance of five recognition methods is analyzed and compared when the standard thermal face representation and the enhanced representation are used. First, a preliminary analysis of the enhanced proposed representation is presented, in particular a selection of the weights of the OWA fusion operator using both the Equinox database and UCHThermalFace database, is given. Secondly, the robustness of the enhanced representation is analyzed in more difficult and realistic scenarios using the UCHThermalFace methodology.

4.1. Preliminary analysis and parameter selection of the OWA operator

We first perform a preliminary analysis of the proposed representation, and also select the weight of the OWA fusion operator using both the Equinox database and UCHThermalFace databases. We compare the use of three representations: Standard thermal representation, vascular image, and proposed enhanced representation. We do this analysis considering the five selected face recognition methods (using the seven best variants obtained in (Hermosilla et al., 2012)), namely LBP-HI-80, GJD-BC, WLD-EU-80, WLD-HI-80, SIFT-L&R-M, SIFT-Lowe-M, and SURF-M.

The performance of the methods was measured using the average of the top-1 recognition rate between all pairs of gallery-test sets, applying the testing methodologies defined by Equinox and UCHThermalFace (see details in Section 4.2 and Section 4.3 respectively). For the UCHThermalFace database, the analysis was performed using only images without variations (Rotation and Speech sets). All Equinox images were normalized following Eq. (10) before performing the anisotropic diffusion. The results are shown in Table 1 and Table 2 for the Equinox and UCHThermalFace databases respectively.

From Tables 1 and 2 it can be observed that the vascular representation alone does not work better than the standard representation, with the exception of GJD-BC and SURF-M in the Equinox database. When the standard and the enhanced representations are compared, the enhanced representation gives better results in terms of the performance improvement with the exception of SIFT and WLD-EU-80 in the UCHThermalFace database, but the difference is small.

When the three considered weighting used in the enhanced representation (w_1=0, w_2=1; w_1=0.1, w_2=0.9; w_1=0.3, w_2=0.7) are compared, the difference among them is rather small, with the exception of w_1=0.3, w_2=0.7 in UCHThermalFace database, which gives just a recognition rate of 69.07% for WLD-EU-80. In the case of UCHThermalFace database, this same variant (w_1=0.3, w_2=0.7) always gives smaller recognition rates when compared to the other two variants (w_1=0, w_2=1; w_1=0.1, w_2=0.9), while these two other variants have almost the same rates. In the Equinox database is not so clear which are best parameters for the OWA operator, with each variant giving best results for least 2 recognition methods.

Table 3. Recognition Rate (%) of the Enhanced Face Recognition Methods in the Different Experiments of the UCHThermalFace Database (See Description in Section 3.1). IN/OUT: Indoor/Outdoor Session.

Method	No Variations		PartialOcclusion		2.5% EyeNoise		5% EyeNoise		10% EyeNoise		GalleryIndoor	GalleryOutdoor	Expression
	IN	OUT	IN	OUT	IN	OUT	IN	OUT	IN	OUT	OUT	IN	IN
e-LBP-HI-80	89.1	88.3	82.8	78.8	89.2	87.5	85.8	85.1	75.8	76.8	25.2	18.8	95.0
e-GJD-BC	95.7	88.7	91.0	81.6	96.2	89.9	94.2	89.5	88.0	75.8	37.0	29.5	95.4
e-WLD-EU-80	91.8	71.9	90.7	67.3	92.3	70.8	89.2	67.1	79.1	60.2	14.9	17.9	94.1
e-WLD-HI-80	96.5	90.2	96.8	90.3	97.6	90.5	95.5	87.6	89.97	79.9	25.1	19.5	94.4
e-SIFT-L&R-M	94.9	94.5	93.3	92.4	95.2	94.2	95.6	94.1	93.8	93.8	11.0	9.1	99.8
e-SIFT-Lowe-M	96.3	94.6	94.4	92.0	96.7	95.7	96.7	94.4	95.9	95.1	11.1	14.6	99.8
e-SURF-M	96.7	95.1	92.8	91.0	96.6	95.3	96.0	93.9	94.5	92.5	19.4	21.8	97.6

Table 4. Improvement of the Recognition Rate ([Δ%]) when using the Enhanced Face Recognition Methods in the Different Experiments of the UCHThermalFace Database (See Description in Section 4.3).

Method	No Variations		PartialOcclusion		2.5% EyeNoise		5% EyeNoise		10% EyeNoise		GalleryIndoor	GalleryOutdoor	Expression
	IN	OUT	IN	OUT	IN	OUT	IN	OUT	IN	OUT	OUT	IN	IN
	[Δ%]	[Δ%]	[Δ%]	[Δ%]	[Δ%]	[Δ%]	[Δ%]	[Δ%]	[Δ%]	[Δ%]	[Δ%]	[Δ%]	[Δ%]
e-LBP-HI-80	**0.6**	−0.8	**0.5**	**0.1**	**0.6**	−0.3	−1.1	−0.3	**0.9**	**0.3**	**3.4**	**0.7**	**0.1**
e-GJD-BC	**4.3**	**8.3**	**9.4**	**8.8**	**5.1**	**8.9**	**5.3**	**9.8**	**8.9**	**5.0**	**1.2**	**0.7**	**1.0**
e-WLD-EU-80	0.0	−1.8	**0.7**	−2.2	−0.3	−2.2	**0.7**	−1.3	−1.1	**0.2**	−4.4	−4.6	**0.2**
e-WLD-HI-80	**4.9**	**0.0**	**5.0**	**4.7**	**7.6**	**5.7**	**8.4**	**4.3**	**11.6**	**5.6**	−3.9	**1.1**	**0.3**
e-SIFT-L&R-M	−0.2	−1.3	**2.7**	0.0	−0.2	−1.8	**0.4**	−0.1	−0.6	0.0	**0.3**	−5.7	**0.9**
e-SIFT-Lowe-M	−1.3	−1.7	−0.1	−2.3	−0.3	−1.3	−1.2	−2.8	−1.0	−1.6	−0.8	**1.6**	**0.2**
e-SURF-M	**2.6**	−0.5	**5.3**	−0.7	**2.8**	−0.3	**3.0**	−1.2	**1.8**	−1.6	−1.8	**1.7**	**10.4**

The comparison is done with respect to the situation in which the standard methods are used. [Δ%] indicates the recognition rate of the enhanced face recognition method minus the recognition rate of the method that uses the standard face representation. In/out: indoor/outdoor session. Positive values, i.E. Cases where the enhanced variant works better, are shown in bold letters.

From these results it can be also observed that the methods that benefit the most when using the enhanced representation are GJD-BC, SIFT, and SURF, in particular in the Equinox database (see the high values obtained by the performance improvement in Table 1). The LBP method is mostly not affected (it presents a small positive improvement by the use of the enhanced representation), while the SIFT-based methods slightly decrease their performance. In summary, in most cases the use of the enhanced representation improves the performance of the recognition methods and the largest improvements are obtained when this representation is used together with the GJD-BC, SIFT-X, WLD-X, and SURF-M methods.

Given that the preliminary results (enhanced and performance improvement) show that using and $w_1 = 0$ gives good results for most methods in the two databases, in the following these values will be used in the evaluation of the robustness of the method using the UCHThermalFace database. Note that this is equivalent to using the maximum operator. Nevertheless, we want to stress that using other values of w_i might give better results for some of the presented methods. Searching for the optimal values for a particular method is out of the scope of the present work. However, it might be worth doing this when a particular recognition method has been selected for a given application.

4.2. Experiments using enhanced thermal representation on the UCH thermal face database

In the following we analyze the robustness of the enhanced representation using the UCHThermalFace database and the methodology used in (Hermosilla et al., 2012). In the experiment we only consider the case w_1=0, w_2=1, and the same recognition methods as before.

Tables 3 and 4 summarize the result of applying the enhanced thermal representation to the face recognition methods under comparison. Table 3 shows the recognition rate obtained by the enhanced face recognition methods in the experiments described in Section 4.3. Table 4 presents the difference in recognition rate obtained by the enhanced face recognition methods versus using the standard representation. In Table 4, a positive value (shown in bold letters) indicates that the improved thermal representation works better for that particular method. The observed results can be summarized as:

A. **Baseline case (no variations applied to the images).** From Table 4 it can be observed that the use of the enhanced thermal representation gives better results for most methods in indoors, showing a slight decrease for SIFT-based methods, and clear improvements for GJD-BC, WLD-HI-80, and SURF-M. In the outdoor case, the use of the enhanced thermal representation gives better results for GJD-BC, but in the other methods the use of the enhanced representation does not produce any clear improvements.
B. **Partial face occlusion:** In the partial face occlusions experiments most of the methods improve or maintain the recognition rates in the indoor case, while in the outdoor case WLD-EU-80 and SIFT-Lowe-M decrease their performance. GJD-BC and WLD-HI improve largely their performance in indoors and outdoors.
C. **Noise in eyes' position:** A behavior similar to the *partial face occlusion* case is observed.
D. **Indoor** versus **Outdoor galleries**. Similarly to the results reported in (Hermosilla et al., 2012), all methods obtain a very low performance when an indoor

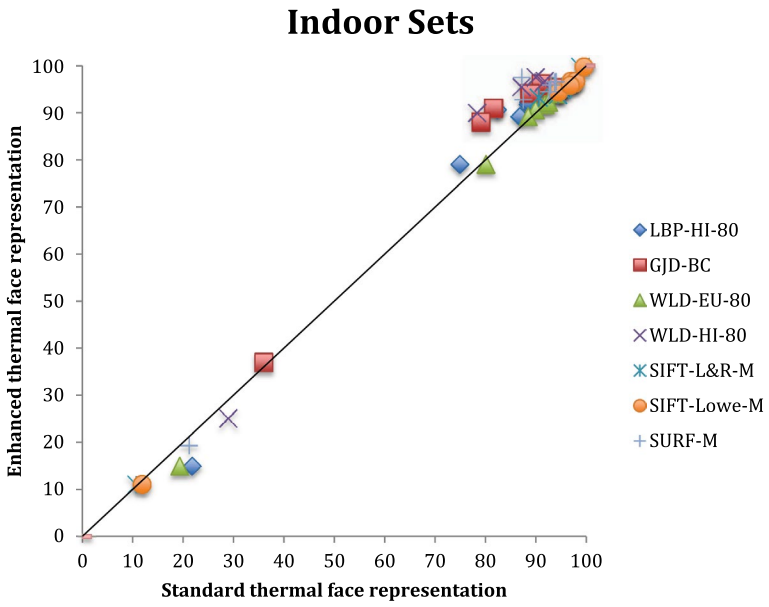

Figure 5. Comparison of Recognition Rates in all Indoor Subsets of the UCHThermalFace Database.
The vertical/horizontal axis corresponds to the recognition rate of the methods when using the enhanced/standard representation. Each point in the figure corresponds to a single experiment (e.G., Partial occlusion) for a single method. Points above the diagonal line indicate that the enhanced representation performs better for the corresponding subset. See main text for details.

gallery set is used with an outdoor test set, or vice versa. The use of the enhanced representation does not produce clear improvements, except for LBP-HI-80, and in some cases the performance of the methods decrease when the enhanced representation is used.

E. **Facial Expression:** The use of the enhanced representation improves the performance of all methods under evaluation. This improvement is small but consistent in all cases, with the exception of SURF-M where there is a large improvement of 10.4%.

4.3. Indoor versus outdoor

It is worth analyzing in more detail the performance of the methods when indoor or outdoor sessions are considered. In the indoor case, when analyzing the obtained results corresponding to all methods and all experiments, it can be observed that by using the enhanced representation, in average, an improvement of 1.89 percentage points in the recognition rate is obtained, with a standard deviation of 1.37; in the outdoor case there is an improvement of 0.75 percentage points in average, with an standard deviation of 0.76. When considering all outdoor experiments, the methods that improve the most with the use of the enhanced representation are GJD-BC with a 6.9% average increase and WLD-HI-80 with a 3.6% average increase. In the indoor case the largest improvements correspond to GJD-BC with a 5.0% average increase, WLD-HI-80 with a 4.9% average increase, and SURF-M with a 3.4% average increase.

Furthermore, in Figure 5 and 6 we present the results of Table 4 in a graphical way for the indoor and outdoor sessions respectively. In these Figures, the vertical axis corresponds to the recognition rate of the methods when the enhanced representation is used, while the horizontal axis shows the recognition rate when a standard representation is employed. Each point in the figure corresponds to a single experiment (e.g., Partial Occlusion) for a single method. Points above the diagonal line indicate that the enhanced representation performs better for the corresponding subset. From Figure 5 (indoor case), it can be observed that in most cases the recognition process using the enhanced representation performs better or the same than using the standard representation. Thus, the use of the enhanced representation performs clearly better for GJD-BC, WLD-HI-80, and SURF-M. From Figure 6 it can be observed a larger dispersion in the results in the outdoor case. Again, the recognition rate clearly increases for the GJD-BC, WLD-HI-80 and SURF-M cases.

5. Discussion and conclusions

Thermal face recognition has attracted increasing interest in the research community in recent years. Existing standard recognition methods still need to be adapted, improved and evaluated when applied to thermal images. In this context, the main goal of this paper is to present a new methodology that allows improving existing thermal face recognition methods by using an enhanced representation of the thermal face images, and in particular any standard face recognition method can be used without any modification. This new representation is obtained by combining the pixels of the thermal face image and the vascular network information extracted from the same thermal face image. Thus, this new representation enhances vascular facial information of the input thermal image. Although in this work we only combine the vascular information with the thermal image, the proposed fusion operator and framework can be easily used together with other sources of information, such as depth images, other infrared bands, and/or visual images.

The proposed methodology was evaluated using two publicly available databases (namely, Equinox and UCHThermalFace), using the same experimental setup, implementations as in previous works. Results show that in many cases the use of the enhanced representation improves the performance of the recognition methods, and that the largest improvements are obtained when this representation is used together with the GJD-BC, WLD-HI, and SURF-M methods. Apparently the LBP method does not require the use of the proposed representation, because it tends to marginally increase the

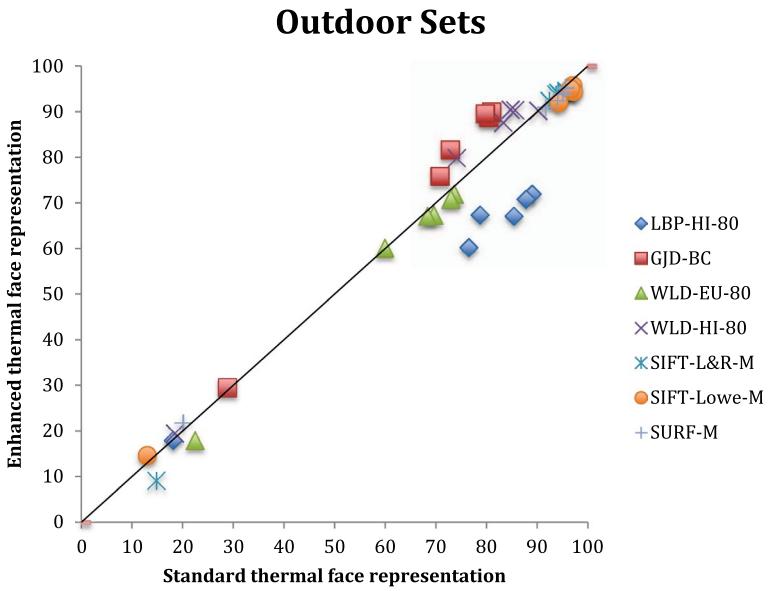

Figure 6. Comparison of Recognition Rates in all Outdoor Subsets of the UCHThermalFace Database.
The vertical/horizontal axis corresponds to the recognition rate of the methods when using the enhanced/standard representation. Each point in the figure corresponds to a single experiment (e.G., Partial occlusion) for a single method. Points above the diagonal line indicate that the enhanced representation performs better for the corresponding subset. See main text for details.

recognition result obtained by using only the standard thermal face representation and its performances slightly decreases in outdoor settings. Furthermore, for the SIFT method does not improve, and most times it slightly decreases its recognition performance when using the proposed enhanced representation. We think this may be due to the way the gradients and interest points are calculated in the SIFT method, which may be affected by the way the vascular network and the thermal face image are fused.

The results obtained when evaluating in the UCHThermalFace database are fully concordant with the ones obtained when the Equinox database was used, except for the case of the WLD-EU method. In Equinox the use of the enhanced representation allows an improvement of 5% for this method, while in the UCHThermalFace case a slightly decrease in the performance is observed. The GJD-BC and WLD-HI methods improve recognition in large percentages. SURF also improves considerably.

Specifically for UCHThermalFace database it was observed that in general terms the improvement is higher in indoor setups than in outdoors. In particular, when experiments were performed indoor and outdoor, a consistency in the results is observed, since the GJD-BC and WLD variants improve significantly more than the other methods of recognition. For outdoor GJD-BC obtains a high performance by increasing the rates obtained from the indoor experiments. Furthermore, the results of indoor are better than outdoor. This seems to be because in indoors the thermal information is more stable (more stable metabolic and environment conditions), but on the other hand outdoor thermal image are more likely affected by factors such as exposure of the face to the sun, the calibration of the thermal camera and the ambient temperature.

In (Hermosilla et al., 2012) was observed that the best performing method, without taking into account the processing speed, was SIFT, and followed by SURF. However, if we compare e-SURF with SIFT (or with e-SIFT), we observe that e-SURF obtains a slightly lower performance than SIFT, but at a higher processing speed (see processing speed information of the methods in (Hermosilla et al., 2012)). Therefore, e-SURF should be preferred over SIFT and e-SIFT, for its higher speed. In (Hermosilla et al., 2012) was also observed that LBP was the fastest method and that best trade-off in terms of processing speed and recognition rate was obtained by WLD-HI-80, followed by LBP. If now the enhanced variants of the methods are considered, e-WLD-HI-80 obtains even higher recognition rates compared to LBP and e-LBP variants. Therefore, we can say that for most applications e-WLD-HI-80 presents the best tradeoff between processing speed and recognition rate and should be preferred.

In summary, it can be observed that in most cases the use of the enhanced representation improves the performance of some of the analyzed recognition methods, and that the largest improvements are obtained when this representation is used together with the GJD-BC, WLD-HI, and SURF-M methods. It can be also observed that in general terms the improvement is higher in the indoor sets than in the outdoor sets.

Notes

1. In the following we will refer to "vascular network information", "vascular network", or "extracted vascular network" indistinctively, even if the obtained representation does not necessarily corresponds the exact vascular network or its topology. See (Pradeep Buddharaju et al., 2008) for an analysis on the extraction of vascular networks from thermal images
2. In all experiments on the UCHThermalFace DB the face images were first aligned using the annotated eyes' position.
3. In these experiments the test and gallery images correspond to images taken in an indoor session or in an outdoor session. When the test images are indoor images, then the gallery images are outdoor-images, and vice versa. The outdoor images were captured in summer (with high temperatures up to 30 degrees Celsius), and at times the faces, as well as the camera, were receiving direct sunlight.

Acknowledgements

This research was partially funded by the FONDECYT-Chile Grants 11130466, 3120218 and 1130153.

Disclosure statement

No potential conflict of interest was reported by the authors.

Notes on contributors

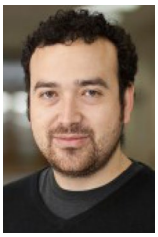

Gabriel Hermosilla received the degree in Electronic Engineering from the University of La Frontera, Temuco, Chile, in 2007. In 2012, he obtained the Ph.D. degree in Electric Engineering from University of Chile, Santiago, Chile. Actually, he is an associate professor in the School of Electrical Engineering at Pontificia Universidad Católica de Valparaiso (PUCV), Valparaiso, Chile. His principal areas of research are thermal face recognition, pattern recognition, and computer vision.

Javier Ruiz-del-Solar received his degree in Electrical Engineering from the UTFSM (Chile) in 1991, and the Doctor-Engineer degree from the Technical University of Berlin in 1997. Since 2009 he is Executive Director of the AMTC Center at the Universidad de Chile. His research interests include Mobile Robotics, Computer and Robot Vision.

Rodrigo Verschae received MSc. in Applied Mathematics in 2006 (Ecole Normale Superieure de Cachan, France) and his Doctoral degree in 2010 (Universidad de Chile, Chile). Currently his is an Assistant Professor at the Graduate School of Informatics, Kyoto University. His research interests include computer vision, pattern recognition, and machine learning.

References

Ahonen, T., Hadid, A., & Pietikainen, M. (2006). Face description with local binary patterns: Application to face recognition. *IEEE Transactions on Pattern Analysis and Machine Intelligence, 28*, 2037–2041.

Bay, H., Ess, A., Tuytelaars, T., & Van Gool, L. (2008). Speeded-up robust features (SURF). *Computer Vision and Image Understanding, 110*, 346–359.

Bebis, G., Gyaourova, A., Singh, S., & Pavlidis, I. (2006). Face recognition by fusing thermal infrared and visible imagery. *Image and Vision Computing, 24*, 727–742.

Buddharaju, P., & Pavlidis, I. (2007). Multispectral face recognition: Fusion of visual imagery with physiological information. In *Face biometrics for personal identification, Multi-Sensory Multi-Modal Systems*, eds. R. I. Hammoud, B. R. Abidi and M. A. Abidi (pp. 91–108). Springer.

Buddharaju, P., Pavlidis, I., & Manohar, C. (2008). Face recognition beyond the visible spectrum. In *Advances in Biometrics: Sensors, Algorithms and Systems*, (pp. 157–180). Springer.

Buddharaju, P., Pavlidis, I., & Tsiamyrtzis, P. (2006). *Pose-invariant physiological face recognition in the thermal infrared spectrum*. Paper presented at the Computer Vision and Pattern Recognition Workshop. CVPRW'06. Conference on.

Buddharaju, P., Pavlidis, I. T., & Tsiamyrtzis, P. (2005). *Physiology-based face recognition*. Paper presented at the Advanced Video and Signal Based Surveillance. AVSS 2005. IEEE Conference on.

Chen, X., Flynn, P. J., & Bowyer, K. W. (2003). *PCA-based face recognition in infrared imagery: Baseline and comparative studies*. Paper presented at the Analysis and Modeling of Faces and Gestures. AMFG 2003. IEEE International Workshop on.

Chen, J., Shan, S., He, C., Zhao, G., Pietikainen, M., Chen, X., & Gao, W. (2010). WLD: A robust local image descripto. *IEEE Transactions on Pattern Analysis and Machine Intelligence, 32*, 1705–1720.

Cho, S.-Y., Wang, L., & Ong, W. J. (2009). *Thermal imprint feature analysis for face recognition*. Paper presented at the Industrial Electronics. ISIE 2009. IEEE International Symposium on.

Desa, S. M., & Hati, S. (2008). *IR and visible face recognition using fusion of kernel based features*. Paper presented at the Pattern Recognition. ICPR 2008. 19th International Conference on.

Equinox. (2012). Equinox Database. Retrieved January 2012, from http://www.equinoxsensors.com/products/HID.html

Evans, C. (2009). OpenSURF library from Matlab. Retrieved October 2011, from http://www.mathworks.com/matlabcentral/fileexchange/28300-opensurf-including-image-warp

Gade, R., & Moeslund, T. B. (2014). Thermal cameras and applications: A survey. *Machine Vision and Applications, 25*, 245–262.

Ghiass, R. S., Arandjelovic, O., Bendada, H., & Maldague, X. (2013a). *Illumination-invariant face recognition from a single image across extreme pose using a dual dimension AAM ensemble in the thermal infrared spectrum*. Paper presented at the Neural Networks (IJCNN), The 2013 International Joint Conference on.

Ghiass, R. S., Arandjelovic, O., Bendada, H., & Maldague, X. (2013b). Vesselness features and the inverse compositional AAM for robust face recognition using thermal IR. *arXiv preprint arXiv:1306.1609*.

Hanmandlu, M. (2014). Robust authentication using the unconstrained infrared face images. *Expert Systems with Applications, 41*, 6494–6511.

Hermosilla, G., Ruiz-del-Solar, J., Verschae, R., & Correa, M. (2012). A comparative study of thermal face recognition methods in unconstrained environments. *Pattern Recognition, 45*, 2445–2459.

James, A. P., & Dasarathy, B. V. (2014). Medical image fusion: A survey of the state of the art. *Information Fusion, 19*, 4–19.

Jones, M. J., & Rehg, J. M. (2002). Statistical color models with application to skin detection. *International Journal of Computer Vision, 46*, 81–96.

Lowe, D. G. (2004). Distinctive image features from scale-invariant keypoints. *International Journal of Computer Vision, 60*, 91–110.

Mangai, U. G., Samanta, S., Das, S., & Chowdhury, P. R. (2010). A survey of decision fusion and feature fusion strategies for pattern classification. *IETE Technical Review, 27*, 293–307.

Mendez, H., San Martin, C., Kittler, J., Plasencia, Y., & Garcia-Reyes, E. (2009). Face recognition with LWIR imagery using local binary patterns, Advances in Biometrics, Volume 5558 of the series http://link.springer.com/bookseries/558. Lecture Notes in Computer Science, (pp. 327–336). Springer.

Mostafa, E., Hammoud, R., Ali, A., & Farag, A. (2013). Face recognition in low resolution thermal images. *Computer Vision and Image Understanding, 117*, 1689–1694.

Nigam, I., Vatsa, M., & Singh, R. (2015). Ocular biometrics: A survey of modalities and fusion approaches. *Information Fusion, 26*, 1–35.

Pop, F. M., Gordan, M., Florea, C., & Vlaicu, A. (2010). *Fusion based approach for thermal and visible face recognition under pose and expresivity variation*. Paper presented at the Roedunet International Conference (RoEduNet), 2010 9th.

Qi, H., & Diakides, N. A. (2009). Thermal infrared imaging in early breast cancer detection - A survey of recent research. In *Augmented Vision Perception in Infrared, Advances in Pattern Recognition* (pp. 139–152). Springer.

Ruiz-del-Solar, J., Loncomilla, P., & Devia, C. (2007). A new approach for fingerprint verification based on wide baseline matching using local interest points and descriptors. In *Advances in Image and Video Technology, Lecture Notes in Computer Science, Volume 4872* (pp. 586–599). Springer.

Ruiz-del-Solar, J., Verschae, R., & Correa, M. (2009). Recognition of faces in unconstrained environments: A comparative study. *EURASIP Journal on Advances in Signal Processing*, special issue, Recent Advances in Biometric Systems: A Signal Processing Perspective, Vol 2009 (pp. 1–19).

Shoja Ghiass, R., Arandjelović, O., Bendada, A., & Maldague, X. (2014). Infrared face recognition: A comprehensive review of methodologies and databases. *Pattern Recognition, 47*, 2807–2824.

Socolinsky, D., Wolff, L. B., Neuheisel, J. D., & Eveland, C. K. (2001). *Illumination invariant face recognition using thermal infrared imagery*. Paper presented at the Computer Vision and Pattern Recognition. CVPR 2001. Proceedings of the 2001 IEEE Computer Society Conference on.

Socolinsky, D. A., & Selinger, A. (2002). A comparative analysis of face recognition performance with visible and thermal infrared imagery. In Proc. Int. Conf. Pattern Recognition (ICPR), Quebec (pp. 217–222).

Socolinsky, D. A., & Selinger, A. (2004). *Thermal face recognition over time*. Paper presented at the Pattern Recognition. ICPR 2004. Proceedings of the 17th International Conference on.

UCHThermalFace. (2014). UCHThermalFace Database. Retrieved January 2014, from http://vision.die.uchile.cl/dbThermal

Vidas, S., Moghadam, P., & Bosse, M. (2013). *3D thermal mapping of building interiors using an RGB-D and thermal camera*. Paper presented at the Robotics and Automation (ICRA), 2013 IEEE International Conference on.

Wong, W. K., Tan, P. N., Loo, C. K., & Lim, W. S. (2009). *An effective surveillance system using thermal camera*. Paper presented at the Signal Acquisition and Processing. ICSAP 2009. International Conference on.

Yager, R. R. (1988). On ordered weighted averaging aggregation operators in multicriteria decisionmaking. *IEEE Transactions on Systems, Man, and Cybernetics, 18*, 183–190.

Zheng, Y. (2010). A novel thermal face recognition approach using face pattern words. Proc. SPIE 7667, Biometric Technology for Human Identification VII, 766703 (April 14, 2010); doi:10.1117/12.850664

Zheng, Y., & Elmaghraby, A. (2011). *A brief survey on multispectral face recognition and multimodal score fusion*. Paper presented at the Signal Processing and Information Technology (ISSPIT). IEEE International Symposium on.

Zou, J., Ji, Q., & Nagy, G. (2007). A comparative study of local matching approach for face recognition. *IEEE Transactions on Image Processing, 16*, 2617–2628.